Journal of Engineering Mathematics (2006) 54: 1–15
DOI 10.1007/s10665-004-7788-1

Suppression of motion-induced residual vibration of a cantilever beam by input shaping

T.-S. YANG*, K.-S. CHEN, C.-C. LEE and J.-F. YIN
*Department of Mechanical Engineering, National Cheng Kung University, 1 University Road, Tainan, Taiwan 701, R.O.C.; *Author for correspondence (E-mail: tsyang@mail.ncku.edu.tw)*

Received 14 May 2004; accepted in revised form 9 December 2004

Abstract. Input shaping is an effective means for suppressing motion-induced residual vibration of lightly damped structures. Here, to demonstrate the ideas of various input shaping schemes for continuous structures, the model system of a cantilever beam, whose base is to be displaced by a prescribed distance, is considered. The cantilever-beam motion is modeled by the damped Bernoulli-Euler beam equation, and is then decomposed into normal vibration modes. For the particular system set up here, the modal equations of motion are linear and uncoupled, and consequently are integrated analytically. It is then shown that, by completing the cantilever base movement in a series of properly calculated steps (*i.e.*, by *shaping* the *input* command of the dynamical system), so as to annihilate the dominant vibration modes through destructive interference, the overall induced vibration of the cantilever can be significantly suppressed. In particular, the "zero-vibration" (ZV) and "zero-vibration-and-derivative" (ZVD) input shaping schemes previously proposed for discrete systems are adapted and applied to the continuous beam here. The theoretical results are also supported by experiments.

Key words: cantilever beam, input shaping, residual-vibration suppression

1. Introduction

The performance of precision machines largely depends on the damping capability of the system in question. This makes damping enhancement an important practical issue in the design of high performance mechanical structures. Basically, the damping capability of a mechanical system can be enhanced by passive and/or active means. In the passive approach, system damping is increased by deploying discrete external dampers such as dashpots, or by integrating a viscoelastic material with a structure member so that the member becomes a "shear damper" [1, Chapter 3]. On the other hand, in the active approach, structural damping can be enhanced by exploiting adaptive materials (*e.g.*, piezoelectric materials) and feedback control [1, Chapter 6].

A third approach to reducing motion-induced residual vibration of elastic structures is to properly administer the input command of the system, *i.e.*, to make use of "input shaping". The idea of shaping the system input to improve its performance has been proposed for decades. Especially during the past ten years or so, extensive research of input shaping has been conducted in robotics and flexible arm control [2–5]. In such studies, the system dynamics typically is modeled by equivalent linearized equations of motion having single or low degrees of freedom; and input-shaping schemes resulting in "zero vibration" (ZV) and "zero vibration and derivative" (ZVD) are developed based on such linear discrete models. Briefly, the ZV scheme decomposes the overall system input into two intermediate steps, each of which is applied at a properly calculated instant, so that the partial system responses to each of the steps interact destructively, thereby suppressing the residual vibration of the

system. When the overall system input is decomposed into three intermediate steps in the ZVD scheme, both the residual vibration amplitude and the *derivative* of the vibration amplitude with respect to timing error can be made zero simultaneously. Clearly, the ZVD scheme therefore is less sensitive to timing error (and hence generally is more robust in real applications) than the ZV scheme.

In other research areas and applications, such as wave propagation and microelectromechanical systems (MEMS), some work has also been done attempting to improve the system performance by modifying the system input [6–8]. In such studies, the structures or wave systems are inherently continuous and nonlinear, so that the existing input-shaping schemes may not always produce satisfactory results. Therefore, to further our understanding and the applicability of input-shaping, it is necessary to examine the performance of various input-shaping schemes on nonlinear continuous systems.

To that end, we have carried out a series of investigations along two major directions. First, to focus on the effects of system nonlinearities on the performance of input-shaping schemes, Yang *et al.* [9] considered nonlinear systems of single degree of freedom (SDOF). Strictly speaking, for nonlinear SDOF systems, the idea of suppressing residual vibration by exploiting linear destructive interference is no longer applicable. Of course, weak nonlinearities may be viewed as structural perturbations to the system dynamics, and the existing input-shaping schemes (*e.g.*, the aforementioned ZV and ZVD schemes) are expected to work reasonably satisfactorily on such systems. For highly nonlinear systems, however, the design methodology of input-shaping schemes has to be modified. Yang *et al.* [9] thus devised an energy (phase plane) approach to study input shaping for highly nonlinear systems. In that work, input shaping was interpreted from an energy viewpoint, and an efficient methodology of input-shaping design for nonlinear SDOF systems was proposed on the basis of an energy balance. The energy approach has also been successfully applied to design input shapers for an electromagnetically actuated nonlinear structure [10].

Along the second direction, we have also studied input shaping for linear continuous systems. This paper presents some of our analytical and experimental findings in such studies, and thus complements the aforementioned works [9,10]. Specifically, we shall demonstrate here the design methodology of input-shaping schemes for linear continuous structures. In particular, the model system of a cantilever beam is considered, whose base is to be displaced by a prescribed distance. As the cantilever is deformable, residual beam vibration generally would be excited by its base movement. The residual vibration would then persist for some time after the cantilever base reaches its destination position, until internal and/or external dissipative mechanisms eventually consume all the kinetic energy associated with the residual vibration. Residual vibration usually is undesirable, as it would deteriorate the performance of precision machines, for example. Although slower base movement generally would excite less residual vibration, it also has the disadvantage of lengthening the time required to complete the task. The objective here is therefore to administer the cantilever-base movement in a way that minimizes the residual beam vibration without much sacrifice of the task time.

Instead of using lumped SDOF (or low-DOF) models that somewhat over-simplify the system dynamics, here the beam motion will be modeled by the damped Bernoulli-Euler beam equation [11, Section 8.1]. The complete mathematical formulation of the problem is presented in Section 2. It will be shown that, for the particular system setup considered here, the beam motion can be decomposed into normal vibration modes of the cantilever, and the resulting modal equations of motion are uncoupled. We are thus able to obtain closed-form expressions for the modal responses. Using the closed-form modal responses, we shall then proceed to discuss the ideas of input-shaping for continuous systems in Section 3. Specifically,

a class of input shaping schemes equivalent to the ZV and ZVD schemes for discrete systems are used to suppress the dominant vibration modes, thereby significantly reducing the overall residual vibration of the cantilever beam. In Section 4, we shall briefly discuss some experimental results supporting the theoretical calculations. Also, to conclude this paper, a number of concluding remarks will be given in Section 5.

2. Formulation and modal decomposition of beam motion

2.1. Bernoulli-Euler beam model

Consider a linearly elastic cantilever beam of length L; the cross-section of the cantilever has an area A and moment of inertia I, both of which are taken to be constant here. Also, the mass density and Young's modulus of the homogeneous beam material will be denoted by ρ and E, respectively. Suppose, in addition, that an actuator is deployed to displace the base of the cantilever ($X=0$, X being the longitudinal coordinate of the cantilever) through a prescribed distance H.

Here the cantilever is modeled as a Bernoulli-Euler beam [11, Section 8.1]. Meanwhile, to incorporate a simple form of energy dissipation, the cantilever motion is supposed to be restrained by a small distributed viscous damping of strength (viscous force/velocity) B per unit longitudinal length of the beam. Accordingly, the lateral beam deflection $Y(X, T)$ – here assumed to be 'small' – is governed by the linear, damped beam equation

$$\rho A\, Y_{TT} + B\, Y_T + E I\, Y_{XXXX} = 0 \quad (0 < X < L),$$

where T is the time variable, and the subscripts denote partial differentiations.

To bring out dynamical similarity, hereafter we shall use dimensionless variables:

$$t = T/T_0, \quad x = X/L, \quad y = Y/H,$$

where T_0 is a characteristic time scale to be specified below. Accordingly, the dimensionless linear equation governing the cantilever motion reads

$$\mu^2 y_{tt} + b\mu y_t + y_{xxxx} = 0 \quad (0 < x < 1), \tag{1}$$

where

$$\mu^2 = \frac{\rho A L^4}{E I T^2} \quad \text{and} \quad b = \frac{B L^2}{\sqrt{\rho A E I}} \tag{2}$$

are the dimensionless inertia parameter and damping coefficient, respectively. Meanwhile, the boundary conditions are written as

$$y = y_0(t), \quad y_x = 0 \quad (x = 0), \tag{3a}$$

$$y_{xx} = y_{xxx} = 0 \quad (x = 1). \tag{3b}$$

To be consistent with the normalization scheme described above, the prescribed cantilever base movement $y_0(t)$ varies here from zero at $t=0$ to unity at a later instant.

2.2. Normal-mode expansion

Having formulated the mathematical model for the cantilever beam motion due to prescribed base movement, we now proceed to decompose the beam motion into normal vibration modes of the cantilever. As it turns out, the modal equations of motion are uncoupled for

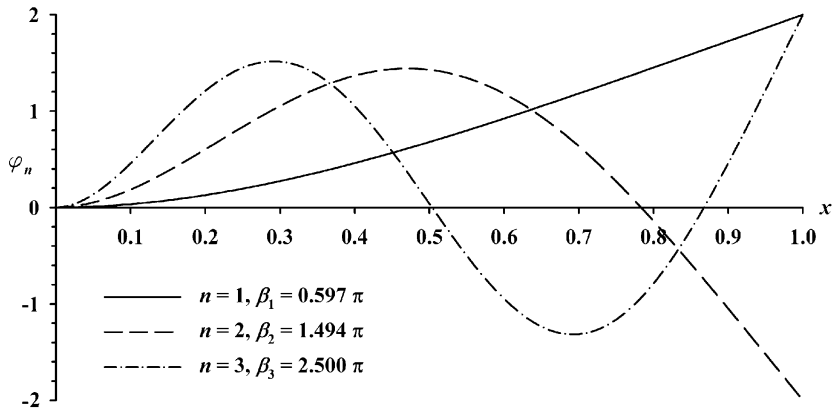

Figure 1. The first three mode shapes of a cantilever beam.

the present system setup, and hence the modal responses can be calculated analytically. This proves convenient for our discussion of input-shaping schemes in the next section.

Note first that free vibration of an undamped cantilever (corresponding to the case $y_0(t) = 0 = b$ in the above formulation) has the normal modes $y_n = \phi_n(x)\exp(i\omega_n t)$ with the mode shapes [11, Section 8.1]

$$\phi_n(x) = \alpha_n\{(\sin\beta_n + \sinh\beta_n)(\cosh\beta_n x - \cos\beta_n x) - (\cos\beta_n + \cosh\beta_n)(\sinh\beta_n x - \sin\beta_n x)\} \quad (n = 1, 2, 3, \ldots), \tag{4}$$

and the corresponding eigenvalues $\beta_n = \sqrt{\mu\omega_n}$ (ω_n being the dimensionless natural frequencies of the cantilever) are the roots of the characteristic equation

$$\cos\beta_n \cosh\beta_n = -1. \tag{5}$$

Here the eigenvalues are numbered in increasing order, so that $0 < \beta_1 < \beta_2 < \beta_3 < \cdots$. Also, the normalization constants α_n are chosen to be

$$\alpha_n = (\sin\beta_n + \sinh\beta_n)^{-1}, \tag{6}$$

so that the normal modes $\phi_n(x)$ $(n = 1, 2, 3, \ldots)$ form an orthonormal basis, *i.e.*,

$$\int_0^1 \phi_m\phi_n \mathrm{d}x = \delta_{mn}, \tag{7}$$

where δ_{mn} is Kronecker's delta.

Figure 1 plots the first three mode shapes; note that, as can be shown, $\phi_n(1) = 2(-1)^{n-1}$. Also, since $\cosh\beta_n \to \infty$ as $n \to \infty$, we deduce from (5) that $\cos\beta_n \to 0$ accordingly, and hence

$$\beta_n \sim (n - 1/2)\pi \quad (n \to \infty). \tag{8}$$

The eigenvalues corresponding to the first three mode shapes are calculated by solving the algebraic Equation (5) numerically, and the results are also listed in Figure 1. It is interesting to note that, even for a mode index as small as $n = 3$, the corresponding eigenvalue (divided by π for convenience, *i.e.*, β_3/π) can be estimated from the above asymptotic formula accurate to the third decimal place.

Now, the characteristic time scale T_0 appearing in the definition of the inertia parameter μ, Equation (2), may be chosen to be the period of the first vibration mode of the cantilever. Accordingly, by definition the dimensionless angular frequency of the first mode

$$\omega_1 = 2\pi; \quad \text{hence} \quad \mu = \beta_1^2/\omega_1 = 0 \cdot 560.$$

Next we expand the beam displacement in terms of the mode shapes:

$$y(x,t) = \sum_{n=1}^{\infty} a_n(t)\phi_n(x), \tag{9}$$

where a_n $(n = 1, 2, 3, \ldots)$ are the modal amplitudes. Substituting the normal mode expansion (9) in (1) yields

$$\mu^2 y_{tt} + b\mu y_t = \sum_{n=1}^{\infty} \left(\mu^2 \frac{\mathrm{d}^2 a_n}{\mathrm{d}t^2} + b\mu \frac{\mathrm{d}a_n}{\mathrm{d}t} \right) \phi_n = -y_{xxxx},$$

and, upon using the orthogonality relation (7), we obtain

$$\mu^2 \frac{\mathrm{d}^2 a_n}{\mathrm{d}t^2} + b\mu \frac{\mathrm{d}a_n}{\mathrm{d}t} = -\int_0^1 \phi_n y_{xxxx} \mathrm{d}x \quad (n = 1, 2, 3, \ldots).$$

Then, integrating the right-hand side of the above equations by parts repeatedly, using the boundary conditions (3) and the fact that $\phi_{nxxxx} = \beta_n^4 \phi_n = \mu^2 \omega_n^2 \phi_n$, we may derive the evolution equations of the modal amplitudes as follows

$$\mu^2 \frac{\mathrm{d}^2 a_n}{\mathrm{d}t^2} + b\mu \frac{\mathrm{d}a_n}{\mathrm{d}t} + \mu^2 \omega_n^2 a_n = \nu_n y_0(t) \quad (n = 1, 2, 3, \ldots), \tag{10}$$

where the parameters

$$\nu_n = -\phi_{nxxx}(0) = 2\alpha_n \beta_n^3 (\cos \beta_n + \cosh \beta_n) \tag{11}$$

may be interpreted as the participation coefficients of the system input (*i.e.*, the base movement $y_0(t)$) for each of the normal modes. Note also that, in view of the asymptotic eigenvalue distribution (8), and using (6), it can be deduced from (11) that $\nu_n \sim 2\beta_n^3$ $(n \to \infty)$.

Unlike the lumped SDOF models widely used in previous studies, here the beam motion has been systematically decomposed into an infinite number of modes, and thus essentially has infinite degrees of freedom by contrast. Moreover, as it turns out, due to the simplicity of the current system setup, the normal modes are uncoupled, and we can proceed to solve the modal equations of motion (10) analytically. Specifically, suppose that the cantilever is initially at rest and its base undergoes a unit-step movement $y_0(t) = H(t)$, where $H(t)$ is the Heaviside's step function; the modal responses are then found to be

$$a_n(t) = \nu_n \beta_n^{-4} \left\{ 1 - \mathrm{e}^{-bt/2\mu} \left(\cos \omega_n' t + \frac{b}{2\mu\omega_n'} \sin \omega_n' t \right) \right\} \quad (n = 1, 2, 3, \ldots), \tag{12}$$

where $\omega_n' = \omega_n (1 - b^2/4\beta_n^2)^{1/2}$ are the natural frequencies of the damped cantilever. Also, during the reviewing process of this paper, an anonymous reviewer kindly pointed out that there is an elegant expression for the amplitude factors $\nu_n \beta_n^{-4}$ appearing in (12):

$$\nu_n \beta_n^{-4} = \frac{2}{\beta_n} \cdot \frac{(-1)^{n+1} \sin \beta_n}{1 + (-1)^n \cos \beta_n}.$$

In the next section, we shall discuss input shaping design for continuous mechanical structures based on the unit step modal responses (12). It is worth mentioning, however, that for more sophisticated (and perhaps more realistic, too!) system setups with payload and/or dissipative mechanisms other than the distributed viscous damping considered here, the normal modes generally would then be coupled. As a result, the modal responses will be affected by the interactions of the normal modes, and the analysis naturally will be more intricate. That, however, is beyond the scope of this paper, and will not be further pursued in this article.

3. Input-shaping schemes

3.1. ZV SHAPER: UNDAMPED SYSTEMS

To gain some insight into input shaping, let us first consider the special case in which dissipative effects are negligible. Accordingly, the damping coefficient $b=0$ in (12), and the modal responses to a unit-step input simplify to

$$a_n(t) = \nu_n \beta_n^{-4}(1-\cos\omega_n t) \quad (n=1,2,3,\dots). \tag{13}$$

It is seen that the modal amplitudes a_n oscillate about their mean values $\nu_n\beta_n^{-4}$, and it can be shown that $\sum_{n=1}^{\infty}\nu_n\beta_n^{-4}\phi_n(1)=1$, so that the cantilever tip oscillates about its target destination $y=1$. Also, from (13) we deduce that the residual vibration of the n-th mode has an angular frequency of ω_n and amplitude $\nu_n\beta_n^{-4}$. Moreover, from the asymptotic eigenvalue distribution (8) and the parameter definition (11), it can be readily shown that the amplitudes of residual vibration are given by

$$\nu_n\beta_n^{-4} \sim \frac{2}{\beta_n} \sim \frac{2}{n\pi} \quad (n\to\infty),$$

and decrease monotonically with the modal index n.

Suppose now that we wish to suppress one of the vibration modes to reduce the overall residual vibration. (A natural choice would be the first mode, since it has the largest amplitude among all modes.) One way to do that is to apply the system input in two steps of equal stroke, so that mathematically the input command reads

$$y_0(t) = \frac{1}{2}\{H(t)+H(t-\tau)\}, \tag{14}$$

where τ is the time lag of the second step with respect to the first. The modal responses due to the first half-step input are simply one half of those given by (13). Furthermore, since the modal evolution Equations (10) are autonomous and thus are invariant with respect to time shift, the modal responses due to the second half-step input can be readily obtained by shifting the temporal variable in the first half-step responses by τ. In addition, due to the linearity of the current setup, we can simply superimpose the above two partial responses to obtain the overall modal responses, and the result for $t>\tau$ (*i.e.*, after the cantilever base reaches its destination) is

$$a_n(t) = \nu_n\beta_n^{-4}\left\{1-\frac{1}{2}(1+\cos\omega_n\tau)\cos\omega_n t - \frac{1}{2}\sin\omega_n\tau\sin\omega_n t\right\} \quad (n=1,2,3,\dots). \tag{15}$$

We thus see that the residual vibration of the n-th mode now has a cosine component of amplitude $\nu_n\beta_n^{-4}(1+\cos\omega_n\tau)/2$ and a sine component of amplitude $\nu_n\beta_n^{-4}(\sin\omega_n\tau)/2$. The overall

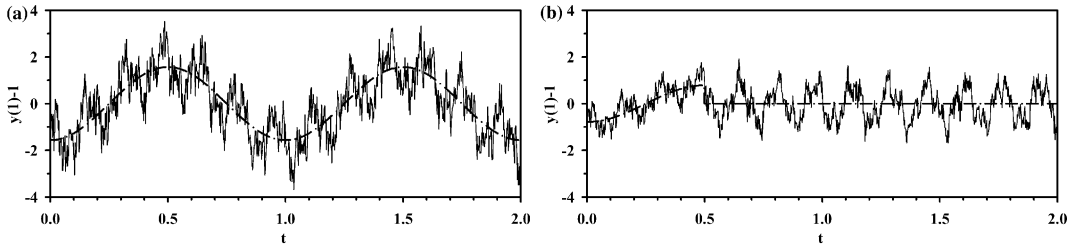

Figure 2. Residual tip vibration of an undamped cantilever undergoing (a) a unit-step base movement $y_0 = H(t)$, and (b) a two-step base movement $y_0 = \{H(t) + H(t - 1/2)\}$, respectively. Solid curves: tip position as a function of time; dot-dashed curves: contributions of the first vibration mode.

modal amplitude therefore is $\nu_n \beta_n^{-4} |\cos(\omega_n \tau/2)|$, and the n-th residual vibration mode is completely suppressed when the time lag between the two half-steps takes one of the values below:

$$\tau = (m + 1/2)\tau_n \quad (m = 0, 1, 2, \ldots), \tag{16}$$

where $\tau_n = 2\pi/\omega_n$ is the dimensionless period of the n-th vibration mode. Recall that we have chosen the characteristic time scale T_0 to be the period of the first mode, hence $\tau_1 = 1$ by definition.

Two-step input-shaping schemes of the form (14) satisfying the zero-vibration (ZV) conditions (16) are referred to as ZV shapers in Singhose's doctoral dissertation [5]. It is clear from the ZV conditions that physically we will be exploiting linear destructive interference between the two partial responses to suppress the residual vibration of the n-th mode. Note that, as a larger value of time lag τ implies a longer time for the cantilever base to settle in its destination, it would be preferable to pick $m = 0$ from the ZV conditions (16). Meanwhile, as noted above, since the first residual-vibration mode typically has the largest amplitude, it would be the natural target to be suppressed in a first attempt of residual-vibration reduction. However, it should be emphasized that complete suppression of one individual mode generally would not completely suppress the infinitely many other modes simultaneously.

To demonstrate these ideas, and the effectiveness of input shaping in residual-vibration reduction, residual tip vibration of an undamped cantilever excited by its base movement is computed by summing up 'all' the modal contributions, and the results are shown in Figure 2. (The total number of vibration modes is chosen such that a further increase of the mode number does not alter the results in Figure 2 appreciably. In practice, however, the temporal resolution of tip-position measurements generally is limited by the instruments being used.) Meanwhile, for clarity of presentation, the contributions of the first vibration mode are also depicted in Figure 2. At any rate, it is seen in Figure 2(a) that, when the cantilever-base movement is completed in one step, the instantaneous amplitude of the residual tip vibration can be as large as four times the base displacement. However, as explained above, in order to suppress the first residual-vibration mode, and thereby reduce the tip vibration to some extent, the base movement may be split into two steps of equal stroke where the second step lags the first by $\tau = 1/2$. The residual tip vibration due to the presence of all the other modes is shown in Figure 2(b), and we see that the maximum instantaneous tip-vibration amplitude is now reduced by a factor of two.

3.2. ZV SHAPER: DAMPED SYSTEMS

Practical mechanical systems more or less are subject to internal and/or external dissipative mechanisms, so here we shall briefly discuss how the above ideas of input shaping should be modified when applied to dissipative mechanical systems.

Again, we may make use of destructive interference and split the base movement into two steps to suppress the n-th residual vibration mode. However, as the modal amplitudes of residual vibration are continuously attenuating, the first partial step must now have a larger stroke than that of the second to compensate for the amplitude attenuation. To be more specific, suppose that the second partial step lags the first by a time τ; then, in view of (12), the first partial step has to be $\exp(b\tau/2\mu)$ times larger than the second, so that at the very instant the second step is applied, the modal amplitudes of the residual vibration thus excited would attenuate to be equal to those excited by the second partial step. Accordingly, requiring that the strokes of the two partial steps add up to unity, the cantilever base movement is calculated to be

$$y_0(t) = \frac{1}{2}\operatorname{sech}\frac{b\tau}{4\mu}\left\{\exp\left(\frac{b\tau}{4\mu}\right)H(t) + \exp\left(-\frac{b\tau}{4\mu}\right)H(t-\tau)\right\}. \tag{17}$$

Now, making use of the linearity and time-shift invariance of the modal evolution Equations (10), the modal responses of a damped cantilever due to the two-step base movement described by (17) can be constructed from the damped unit-step responses (12). The results for $t > \tau$ are

$$a_n(t) = \nu_n\beta_n^{-4}\left\{1 - \frac{e^{b\tau/4\mu}}{2}\operatorname{sech}\frac{b\tau}{4\mu}\ e^{-bt/2\mu} \times \left[\left(1 + \cos\omega_n'\tau - \frac{b}{2\mu\omega_n'}\sin\omega_n'\tau\right)\cos\omega_n' t\right.\right.$$
$$\left.\left. + \left(\sin\omega_n'\tau + \frac{b}{2\mu\omega_n'}(1+\cos\omega_n'\tau)\right)\sin\omega_n' t\ \right]\right\} \quad (n = 1, 2, 3, \ldots). \tag{18}$$

Hence the overall modal amplitudes of the residual vibration are calculated (by combining the sine and cosine components) to be

$$A_n(t;\tau) = \nu_n\beta_n^{-4}\left[1 + \left(\frac{b}{2\mu\omega_n'}\right)^2\right]^{1/2} e^{b\tau/4\mu}\ \operatorname{sech}\frac{b\tau}{4\mu}\ \left|\cos\frac{\omega_n'\tau}{2}\right| e^{-bt/2\mu}.$$

Of course, under the action of viscous damping, these amplitudes decay with time.

We may define the 'vibration reduction factors' to be the ratios of the modal amplitudes with input shaping to those without:

$$R_{n,2\text{step}}(\tau; b) \equiv \frac{A_n(t;\tau)}{A_n(t;0)} = e^{b\tau/4\mu}\ \operatorname{sech}\frac{b\tau}{4\mu}\ \left|\cos\frac{\omega_n'\tau}{2}\right| \quad (n = 1, 2, 3, \ldots). \tag{19}$$

(Incidentally, the time-attenuation factor $e^{-bt/2\mu}$ that appears in the modal amplitudes A_n is cancelled out in the reduction factors $R_{n,2\text{step}}$.) We thus see that, if the n-th residual vibration mode is to be suppressed, the time lag between the two partial steps may be chosen to be

$$\tau = (m + 1/2)\tau_n' \quad (m = 0, 1, 2, \ldots), \tag{20}$$

where $\tau_n' = 2\pi/\omega_n'$. Note also that (20) generalizes the undamped ZV conditions (16) by replacing the undamped natural periods τ_n with the damped periods τ_n'.

As an example, taking $b = 0{\cdot}05$ for the dimensionless damping coefficient, the residual tip vibration of a damped cantilever excited by its base movement is computed by summing up the modal contributions. The residual tip vibration excited by a unit-step base movement is shown in Figure 3(a). It is seen that initially the instantaneous tip-vibration amplitude reaches about three times the cantilever-base displacement, but the tip vibration is then slowly attenuated by the weak damping imposed here. In an attempt to reduce the residual tip vibration, the base movement is split into two steps described mathematically by (17), with $\tau = \tau_1'/2$ to

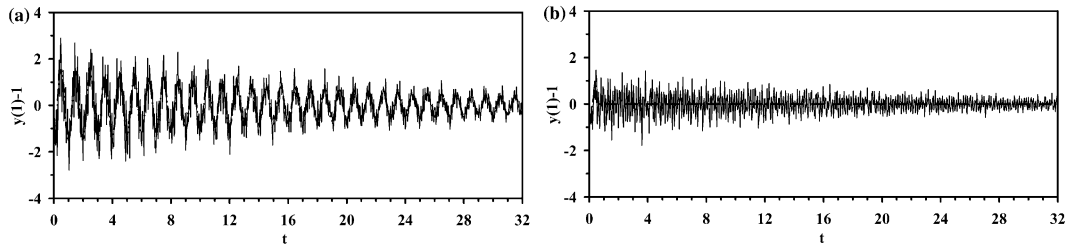

Figure 3. Residual tip vibration of a damped cantilever (taking $b = 0{\cdot}05$) undergoing (a) a unit-step base movement and (b) a two-step base movement described by (17) with $\tau = \tau_1'/2$, respectively. Solid curves: temporal variations of the tip position; dot-dashed curves: contributions of the first vibration mode.

suppress the first residual-vibration mode. The resulting tip vibration is plotted in Figure 3(b). Comparing Figure 3(a) and 3(b), we see that, in spite of the presence of the second and higher residual vibration modes, the residual tip vibration is substantially reduced by the two-step input shaping. Consequently, the time required for the cantilever tip vibration to reduce below a tolerable level will be shortened by use of a two-step input-shaping scheme in the form of (17).

3.3. ZVD SHAPERS

Next let us discuss the potential advantages of using a slightly more sophisticated input-shaping scheme. Specifically, consider first an undamped cantilever whose base movement is completed in three steps:

$$y_0(t) = \frac{1}{4}\{H(t) + 2H(t-\tau) + H(t-2\tau)\}, \tag{21}$$

for which the modal responses for $t > \tau$ can be constructed from (13), yielding

$$a_n(t) = \nu_n \beta_n^{-4} \left\{1 - \frac{1}{2}(1 + \cos\omega_n\tau)\cos\omega_n(t-\tau)\right\} \quad (n = 1, 2, 3, \ldots). \tag{22}$$

We shall explain later how the three-step input-shaping scheme (21) can be deduced. However, as for the modal responses (15) to the two-step input shaping, residual vibration of the n-th mode is completely suppressed when any one of the ZV conditions (16) is met. Physically, under the ZV conditions residual vibration of the n-th mode excited by the first and the third partial steps in (21) would interact constructively, and then jointly annihilate that excited by the second partial step. However, for general values of the time-lag parameter τ, the residual-vibration reduction factor for the n-th mode due to the three-step shaping scheme (21) is

$$R_{n,3\text{step}}(\tau; b = 0) = \frac{1}{2}(1 + \cos\omega_n\tau),$$

in contrast with the two-step reduction factor (see Equation (19))

$$R_{n,2\text{step}}(\tau; b = 0) = |\cos(\omega_n\tau/2)|$$

due to the input-shaping scheme (14).

In Figure 4 we compare the residual-vibration reduction factors $R_{n,3\text{step}}$ and $R_{n,2\text{step}}$. It is seen that the three-step reduction factor has zero slope when it becomes zero under the ZV condition $\tau = \tau_n/2 = \pi/\omega_n$, while the two-step reduction factor has nonzero slope there. (As a matter of fact, $R_{n,2\text{step}}$ reaches its maximum slope there instead). For this reason, the three-step input-shaping scheme (21) is referred to as the ZVD shaper by Singhose [5]. From

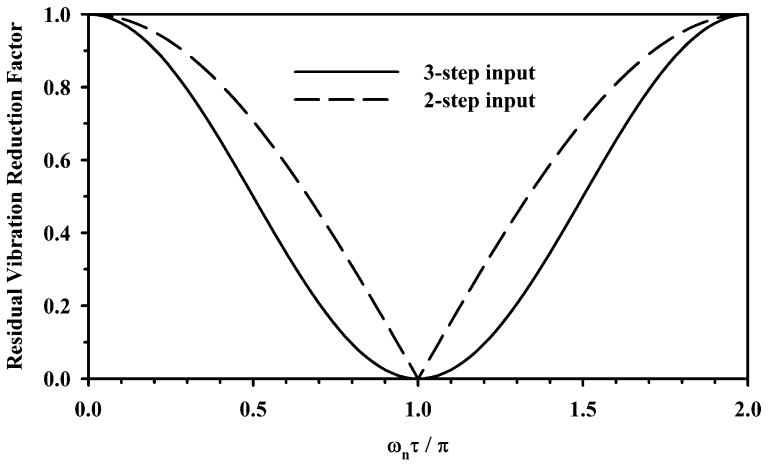

Figure 4. Comparison of the residual vibration reduction factor for the n-th mode due to the three-step input-shaping scheme (21) with that due to the two-step input-shaping scheme (14).

a practical perspective, it would be somewhat difficult to fine-tune the time-lag parameter τ to satisfy the ZV condition $\tau = \tau_n/2 = \pi/\omega_n$ exactly. So, the fact that the three-step input-shaping scheme (21) has a wider window of small vibration amplitude near the ZV time lag $\tau = \pi/\omega_n$ than the two-step scheme (14), clearly is an advantageous feature, for it renders the effectiveness of residual-vibration reduction less sensitive to the value of the time-lag parameter τ. Of course, the trade-off here is the longer time required for the cantilever base to reach its destination position in the three-step scheme than that in the two-step scheme. However, as will be discussed below, the increase in the overall task time typically is much shorter than the settling time of the system, and therefore is relatively insignificant.

Having seen the advantage of the ZVD input shaper over the ZV shaper, we now easily understand how the ZVD shaper (21) can be deduced. In fact, it is straightforward to calculate the resulting vibration amplitude of a three-step input in which the three partial steps are equally spaced in time by τ as in (21), but each has an arbitrary magnitude. Of course, by scaling the three partial-step magnitudes must add up to unity. Furthermore, as our objective is to reduce the sensitivity of the residual-vibration amplitude with respect to timing error under ZV conditions, the derivative of the vibration amplitude with respect to the time spacing τ therefore is set to zero at the ZV values of τ. With these constraints, one then readily deduces the ZVD shaper (21).

For a damped cantilever, to take into account the temporal attenuation of the modal responses excited by earlier partial steps, the three-step input-shaping scheme (21) is modified to be

$$y_0(t) = \frac{1}{2}\left(1+\cosh\frac{b\tau}{2\mu}\right)^{-1}\left\{e^{b\tau/2\mu}H(t)+2H(t-\tau)+e^{-b\tau/2\mu}H(t-2\tau)\right\}. \tag{23}$$

Note that the dimensionless strokes of the three partial steps add up to unity, as required by the normalization scheme here. Meanwhile, the modal responses for $t > \tau$ are constructed from the damped unit-step responses (12) to be

$$a_n(t) = \nu_n\beta_n^{-4}\left\{1-\frac{e^{b\tau/2\mu}(1+\cos\omega_n'\tau)}{1+\cosh(b\tau/2\mu)}\ e^{-bt/2\mu}\right.$$
$$\left.\times\left[\cos\omega_n'(t-\tau)+\frac{b}{2\mu\omega_n'}\sin\omega_n'(t-\tau)\right]\right\} \quad (n=1,2,3,\ldots). \tag{24}$$

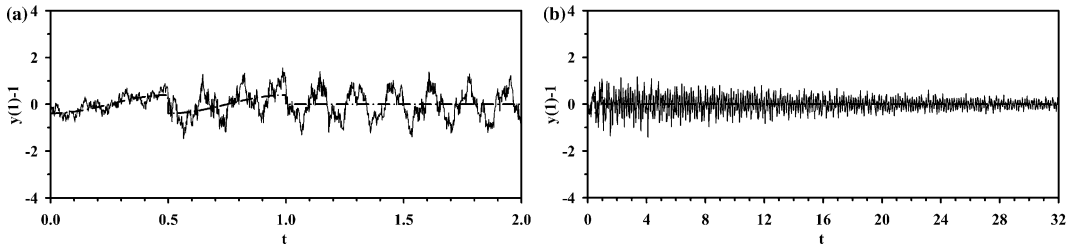

Figure 5. Residual tip vibration of a cantilever excited by three-step base movement. (a) Without damping; the base movement is described by (21) with $\tau = 1/2$. (b) With damping coefficient $b = 0{\cdot}05$; the base movement is described by (23) with $\tau = \tau_1'/2$. Solid curves: temporal variations of the tip position; dot-dashed curves: contributions of the first vibration mode.

Hence, comparing (24) with (12), we find that with damping the residual-vibration reduction factor for the n-th mode due to the three-step shaping scheme (23) is

$$R_{n,3\text{step}}(\tau; b) = \frac{e^{b\tau/2\mu}}{1+\cosh(b\tau/2\mu)}\ (1+\cos\omega_n'\tau), \tag{25}$$

in contrast with the two-step reduction factor defined in (19). Of course, the reduction factors reduce to the undamped results given above when the damping coefficient $b \to 0$. So, as damping effects typically are quite weak in elastic structures requiring the use of input shaping, Figure 4 still is an appropriate comparison between the residual-vibration reduction factors $R_{n,3\text{step}}$ and $R_{n,2\text{step}}$. (The damping effects are included in the above general calculations, however, so that the results are expected to be useful for systems having stronger damping as well.) We thus see that both the three-step and two-step reduction factors vanish when one of the ZV conditions (20) for a damped structure is satisfied. However, the three-step (or ZVD) shaper is superior to the two-step (or ZV) shaper in the sense that its effectiveness of residual-vibration reduction is less sensitive to the value of the time-lag parameter τ. Of course, we reiterate here that the trade-off is the slightly longer time required for the cantilever base to reach its destination position when the ZVD shaper is employed.

To demonstrate the effectiveness of the ZVD shaper in residual-vibration reduction, the tip motion of a cantilever is calculated by summing up the modal contributions. In Figure 5(a) we plot the result for an undamped cantilever whose base movement is described by (21) with $\tau = 1/2$ to suppress the first residual-vibration mode. Meanwhile, the result for a damped cantilever (taking $b = 0{\cdot}05$) whose base movement is described by (23) with $\tau = \tau_1'/2$ to suppress the first residual-vibration mode is shown in Figure 5(b). Comparing Figures 5(a) and 2(b), we see that the residual tip vibration caused by the ZVD shaper appears to be slightly smaller in amplitude than that excited by the ZV shaper. Meanwhile, comparison of Figures 5(b) with 3(b) shows that the same is true. This can be understood on physical grounds, since smoothing out the base movement by splitting it into more steps generally would also reduce the spectral amplitudes of the second and higher vibration modes, which constitute the residual vibration in both the ZV and the ZVD cases.

Moreover, note that in the damped cases, Figures 5(b) and 3(b), the time required for the cantilever tip to settle down is mainly controlled by the decay rates of the residual vibration modes, which, in turn, are determined by the damping coefficient b. Therefore, when the damping effects are relatively weak, as is true in all the cases discussed here, the extra time required for the cantilever base to reach its destination position when a ZVD shaper is used would be quite insignificant compared with the total time required for the tip vibration to reduce below an admissible level. In other words, while both the ZVD and ZV input shapers

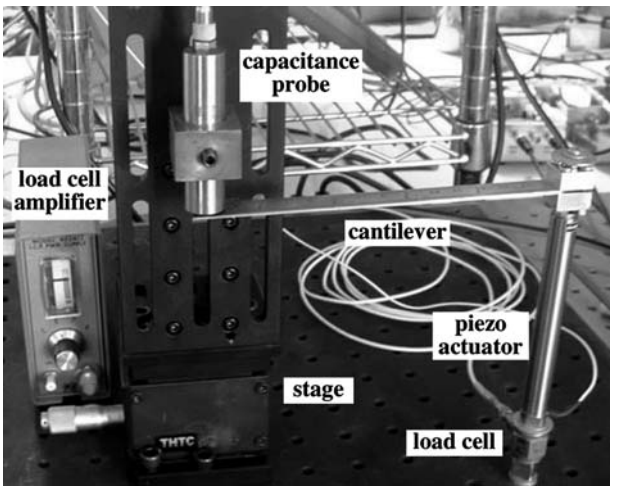

Figure 6. Experimental setup.

suppress the first residual-vibration mode, the overall time required for the cantilever tip to settle down is still somewhat shorter when the ZVD shaper is used. It can then be argued that, compared with the ZV shaper, the ZVD shaper not only is more tolerant of parameter fine-tuning errors in suppressing the main vibration mode, but also reduces the amplitudes of the surviving modes to a greater extent. So, the ZVD input-shaping scheme generally is preferable in practice.

4. Experiments

Here we present some experimental results that demonstrate the effectiveness in residual vibration reduction of the various input-shaping schemes discussed above. For a more detailed discussion of the experimental procedures and results, the reader is referred to the experimentally oriented paper of Chen *et al.* [12].

As shown in Figure 6, the test structure is a stainless-steel beam having a length of 155 mm, width of 13·6 mm, and thickness of 1·2 mm. One end of the beam (the tip of the cantilever) is free to vibrate, while the other end (the base of the cantilever) is clamped on a piezoelectric actuator (Piezo Jena PA100-12, bandwidth $\sim$100 Hz). The base movement of the cantilever is then controlled by digital signals generated by a Pentium III 933 MHz personal computer. A capacitive displacement sensor (MTI ASP50, having a dynamic range of 1·25 mm and bandwidth of 5 KHz) is used to pick up the displacement of the flexural cantilever. Also, the whole system is set on an optical table (DVIO-R-2412M-200t) to isolate it from undesirable environmental vibration.

When a unit-step input is applied to displace the cantilever base by a stroke of about 33 μm, the induced tip vibration initially has a peak-to-peak amplitude of about 83 μm (which is less than three times the base movement). The amplitude is then slowly attenuated, and the dimensionless damping coefficient is estimated to be $b \approx 0{\cdot}025$. Note that here the initial vibration amplitude appears to be much less than that shown in Figure 3(a), where the initial peak-to-peak amplitude is about six times the base displacement. To understand this, note that it takes a finite rise time for a real piezoelectric actuator to execute a 'step input,' in contrast with the zero rise time of the mathematical fiction of $y_0 = H(t)$, and, generally speaking, slowing down the system input command would reduce the excited vibration. In fact, we

have also calculated the residual-vibration amplitude of a cantilever whose base movement is given by $y_0 = [1 - \cos(\pi t/t_r)]/2$ for $0 \le t \le t_r$ and $y_0 = 1$ for $t > t_r$, where t_r is the (dimensionless) finite time the cantilever base takes to reach its destination [13]. As it turns out, the agreement between analytical and experimental results is improved as expected. The algebra involved, however, is somewhat messier than that presented above for a unit-step input, and thus is not discussed in this paper.

Moreover, as the system damping is relatively weak, here we simply use the ZV and ZVD input commands, (14) and (21) respectively, for undamped systems. (For small values of the damping parameter b, the difference between the input commands for systems with and without damping is negligible. Note also that, since input shaping typically is employed for lightly damped structures, oftentimes it suffices to use the simpler commands (14) and (21) for undamped systems, instead of the more general commands (17) and (23) that are expected to be useful for systems subject to stronger damping effects.) Also, from the experiments, the first and second vibration modes are found to have natural frequencies of 40 and 250 Hz, respectively, consistent with the theoretical prediction that $\omega_2/\omega_1 = (\beta_2/\beta_1)^2 = 6{\cdot}25$. The period of the first vibration mode therefore is $T_0 = 25$ ms (recall that T_0 is the characteristic time scale used in the normalization scheme). This result also suggests that a time lag of 12·5 ms (half the first natural period; *i.e.*, $\tau = 1/2$) should be used for both the ZV and ZVD input shapers (14) and (21) to suppress the first residual-vibration mode.

However, for the purpose of comparing the experimental and theoretical results, in the experiments we intentionally vary the time lag parameter τ appearing in the input commands (14) and (21) around 1/2, and estimate the corresponding percentage of the residual tip-vibration amplitude to that excited by the unit-step input. It should be noted that here the peak-to-peak vibration amplitude is estimated using the experimental data obtained within a time interval around a prescribed instant, and the results corresponding to data around 100 and 1250 ms are shown in Figure 7. The theoretical predictions of residual-vibration percentages for a single vibration mode have been shown in Figure 4 above, and are also reproduced in Figure 7 for comparison.

Generally speaking, the experimental results agree well with the uni-modal theoretical predictions, except near the low-vibration windows around $\tau = 1/2$. This is in fact easy to understand on physical grounds, since here the residual vibration actually consists of a large number of detectable modes, so that even if the first mode is completely suppressed, the overall residual-vibration amplitude still is nonzero in general. Note also that, unlike the simple theoretical model used here, each vibration mode is damped to a different extent, and generally speaking modes of higher frequencies suffer a large damping. Therefore, at a later instant, the tip vibration would consist mainly of the first mode, and this is exactly why the agreement between the experimental results and uni-modal theoretical predictions in Figure 7(b) is better than that in Figure 7(a).

An additional interesting feature of Figure 7 is that in some cases, particularly when a longer lag time τ is used for the input commands, the experimental data of vibration amplitude are smaller than the theoretical predictions based on a mathematically idealized unit-step input (having a zero rise time). Again, this can be understood as a consequence of the finite rise time of a real piezoelectric actuator, and the fact that an input command having a longer characteristic time scale generally has a narrower frequency spectrum, resulting in reduced vibration amplitude. (As remarked earlier, close agreement between the analytical and numerical results can be obtained by use of more realistic cantilever base movements in the calculation of the vibration amplitude [13].) Nonetheless, the experimental data indicate that the ZVD shaper not only is more tolerant of parameter fine-tuning errors than the ZV

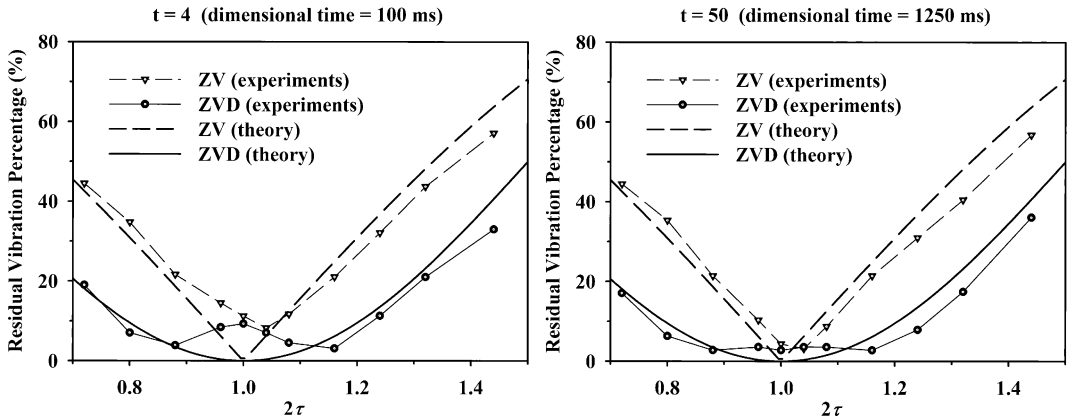

Figure 7. Comparison of experimental and theoretical results at (a) $t=4$ and (b) $t=50$ for both the ZV and ZVD input commands.

shaper in suppressing the main vibration mode, but also reduces the amplitudes of the surviving modes to a greater extent. So, the ZVD input-shaping scheme generally is preferable in practice.

5. Concluding remarks

Here we have demonstrated the main ideas of various input-shaping schemes for continuous structures. In particular, a cantilever beam, whose base is to be displaced by a prescribed distance, is taken to be the model system. Unlike the lumped SDOF models widely used in previous studies, the beam motion is modeled here by the damped Bernoulli-Euler beam equation, and systematically decomposed into an infinite number of normal vibration modes. The system dynamics thus has infinite degrees of freedom.

For the system setup considered in this paper, the modal equations of motion are uncoupled, and hence are integrated analytically. On the basis of the analytic expressions for the modal responses, it is shown that, by completing the cantilever-base movement in a series of intermediate steps so as to annihilate the dominant vibration modes through destructive interference, the overall induced vibration of the cantilever can be significantly suppressed. In particular, the "zero-vibration" (ZV) and ZVD input-shaping schemes previously proposed for discrete systems are adapted and applied to the continuous beam here. Meanwhile, since input shaping typically is employed for lightly damped structures, it usually suffices to use the simpler commands (14) and (21) for undamped systems, instead of the more general commands (17) and (23) that are expected to be useful for systems subject to stronger damping effects.

Comparison of the performances of the ZV and ZVD input-shaping schemes indicates that the ZVD shaper not only is more tolerant of parameter fine-tuning errors than the ZV shaper in suppressing the main vibration mode, but also reduces the amplitudes of the surviving modes to a greater extent. So, the ZVD input-shaping scheme is preferable in practice, and this conclusion is also supported by experimental results.

In closing, we mention that, if in some situations it is desirable to suppress two dominant vibration modes simultaneously, one may incorporate two time lags into the input command to trigger destructive interference of two vibration modes at once. As a specific example, suppose that the first and second modes are to be suppressed, both in a ZVD manner. Then the

input command for an undamped system should be

$$H(t)=\frac{1}{4}\left\{\frac{1}{4}H(t)+\frac{1}{2}H(t-\tau_1/2)+\frac{1}{4}H(t-\tau_1)\right\}$$
$$+\frac{1}{2}\left\{\frac{1}{4}H(t-\tau_2/2)+\frac{1}{2}H(t-\tau_1/2-\tau_2/2)+\frac{1}{4}H(t-\tau_1-\tau_2/2)\right\}$$
$$+\frac{1}{4}\left\{\frac{1}{4}H(t-\tau_2)+\frac{1}{2}H(t-\tau_1/2-\tau_2)+\frac{1}{4}H(t-\tau_1-\tau_2)\right\}.$$

It has been demonstrated by Lee [13] that the above input command not only reduces the residual vibration amplitude to a greater extent than single-mode input-shaping commands do, but also is quite insensitive to timing errors. Of course, by the same token it is also possible to use an even more complicated input command to suppress three or more vibration modes simultaneously, provided that the gain in the effectiveness of residual vibration reduction justifies the added complexity of such input commands.

Acknowledgements

The authors gratefully acknowledge the R.O.C. (Taiwan) National Science Council for supporting this work through Grants NSC90-2212-E006-059, NSC91-2212-E006-082 and NSC92-2212-E006-122.

References

1. J.J. Connor, *Introduction to Structural Motion Control*. Upper Saddle River, NJ: Pearson Education, Inc. (2003) 680pp.
2. L.Y. Pao and M.A. Lau, Robust input shaper control design for parameter variations in flexible structures. *ASME J. Dyn. Syst., Meas., Control* 122 (2000) 63–70.
3. T.-C. Lin, Design an input shaper to reduce operation-induced vibration. In: A.H. Haddad (General Chair), *Proceedings of the 1993 American Control Conference*. Piscataway, NJ: Institute of Electrical and Electronics Engineers (1993) pp. 2502–2506.
4. N.C. Singer and W.P. Seering, Design and comparison of command shaping methods for controlling residual vibration. In: G.A. Bekey (General Chair), *Proceedings of the IEEE International Conference on Robotics and Automation*. Piscataway, NJ: Institute of Electrical and Electronics Engineers (1989) pp. 888–893.
5. W.E. Singhose, *Command Generation for Flexible Systems*. Ph.D. thesis, Department of Mechanical Engineering, Massachusetts Institute of Technology, Cambridge, MA (1997) 285pp.
6. P.F. van Kessel, L.J. Hornbeck, R.E. Meier and M.R. Douglass, MEMS-Based projection display. *Proc. IEEE* 86 (1998) 1687–1704.
7. T.-S. Yang and W.-L. Liang, Suppression of nonlinear forced waves by input shaping. *Wave Motion* 37 (2003) 101–117.
8. S.-P. Su and T.-S. Yang, Suppression of nonlinear forced waves by error-insensitive input shaping. *J. Chinese Soc. Mech. Engng.* 23 (2002) 507–516.
9. T.-S. Yang, K.-S. Chen and J.-F. Yin, Design of input shapers for vibration control in Duffing nonlinear systems. *Mechatronics*, submitted (2004).
10. K.-S. Chen, T.-S. Yang, J.-F. Yin and J.-Y. Chen, Residual vibration suppression for Duffing nonlinear systems with electromagnetic actuation using nonlinear input shaping techniques. *ASME J. Vib. Acost.*, submitted (2004).
11. J.S. Rao, *Advanced Theory of Vibration*. New Delhi (India): Wiley Eastern Ltd. (1992) 431pp.
12. K.-S. Chen, J.-F. Yin, T.-S. Yang and K.-S. Ou, Residual vibration suppression of a piezoelectrically driven cantilever beam by input shaping. *J. Chinese Soc. Mech. Engng.* 25 (2004) 59–67.
13. C.-C. Lee, *Suppression of Motion-Induced Residual Vibration of Continuous Systems by Input Shaping*. MS thesis (in Chinese), Department of Mechanical Engineering, National Cheng Kung University, Tainan, Taiwan (2004) 117pp.